Modelling and Small-Signal Analysis of a Grid Connected Doubly-Fed Induction Generator

Francoise Mei, *Student Member, IEEE*, and Bikash C. Pal, *Senior Member, IEEE*

Abstract—**This paper describes the modeling and small signal analysis of a grid connected doubly-fed induction generator (DFIG). Different models are formulated and compared with each other for different assumptions (two or one-mass drive train, with or without stator transients). The models are developed from the basic flux linkage, voltage and torque equations. Eigenvalues and participation factor analysis of the linearized models are carried out to relate the DFIG electromechanical modes to its relevant state variables.**

Index Terms—**doubly-fed induction generator, non-linear dynamical model, small-signal model, eigenvalue analysis.**

I. INTRODUCTION

WITH the worldwide trend and wish to integrate more wind energy into the power system, there has been an urgent need of suitable dynamical models of wind generators. For the doubly-fed induction generator (DFIG), this resulted in many papers (e.g. [1]-[5]) presenting, in most cases, non-linear dynamical models.

As control design is a major concern, a small-signal analysis can give valuable information on the DFIG properties, limitations and control options. This paper presents the small-signal analysis of a grid connected DFIG. To this end, the system non-linear dynamical model is derived. Then, its linearization and eigenvalue analysis are presented.

In section II, the phase voltage equations of the DFIG are formulated. In sections III-IV, the dq-transformation used in this paper is specified and a dq-model for stability studies is obtained. In sections V-VII, the electromagnetic torque derivation, drive train and converter models are presented. In section VIII, the power flow equations are established to complete the system mathematical model. In section IX, different models are formulated for different sets of assumptions. Finally, in section X, the models are compared with each other with the results of their eigenvalue analysis.

II. DFIG EQUATIONS IN abc-FORM

The convention adopted in this paper for positive current, voltage and flux directions is shown in Fig. 1. As the machine

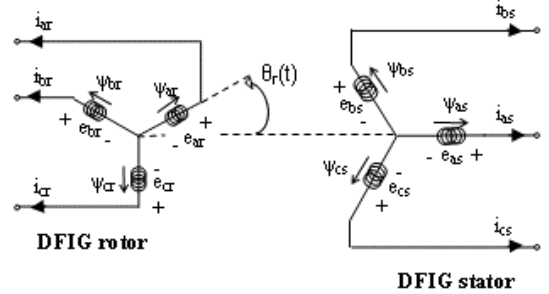is working in generator mode, positive currents are flowing out of it.

Fig. 1. Definition of positive current, voltage and flux directions.

The sign of the self-flux linkage produced by a current in a circuit is the same as that of the current. The polarity of the voltage induced by a changing flux is so that it results in a current that opposes the change (Lenz's law).

Applying the Kirchoff voltage law to Fig. 1 gives:

$$v_{as} = -\frac{1}{\omega_B}\frac{d}{dt}\psi_{as} - R_s i_{as} \tag{1}$$

where R_s, v_{as}, i_{as}, and ψ_{as} are in [pu] and are the stator phase-a winding resistance, voltage, current and flux linkage, respectively; ω_B [rad/sec] is the system base frequency which is equal to the synchronous frequency, i.e. $\omega_B = 2\pi f$; and t is the time in [sec]. In (1), the flux ψ_{as} is:

$$\psi_{as} = \left(L_{self,s} + L_{leak,s}\right)i_{as} + L_{mut,s}\left(i_{bs} + i_{cs}\right) + \dots$$
$$L_{sr}\left(\cos\theta_r i_{ar} + \cos(\theta_r + \frac{2\pi}{3})i_{br} + \cos(\theta_r - \frac{2\pi}{3})i_{cr}\right) \tag{2}$$

where $\theta_r = \theta_r(t)$ is the angle between the stator a-axis (stationary) and rotor a-axis (rotationary) as shown on Fig. 1; $L_{self,s}$ and $L_{leak,s}$ are the self- and leakage inductance of a stator winding, respectively; $L_{mut,s}$ is the mutual inductance between two stator windings; and L_{sr} is the peak value of the mutual inductance between stator and rotor windings. For the other phases of the stator and rotor, similar equations can be written.

III. abc-dq TRANSFORMATION

A. Transformation Matrix

For easier control, three-phase variables are transformed into dq-variables. In matrix notation, we have:

$$v_{qd0} = T_\theta v_{abc} \qquad (3)$$

where $v_{qd0} = [v_q\ v_d\ v_0]'$, $v_{abc} = [v_a\ v_b\ v_c]'$, and T_θ is the abc-to-dq transformation matrix. In this paper, the power invariant transformation is chosen, and the d-axis is leading the q-axis (IEEE recommendation for synchronous machines [9]). Fig. 2 shows the dq-frame with respect to the stator 3-axis frame. The corresponding transformation matrix is given in (4).
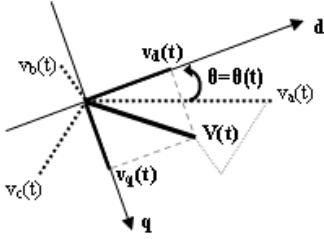

Fig.2. dq-frame with respect to stator abc-frame.

$$T_\theta = \sqrt{\frac{2}{3}} \cdot \begin{pmatrix} \sin\theta & \sin(\theta - 2\pi/3) & \sin(\theta + 2\pi/3) \\ \cos\theta & \cos(\theta - 2\pi/3) & \cos(\theta + 2\pi/3) \\ 1/\sqrt{2} & 1/\sqrt{2} & 1/\sqrt{2} \end{pmatrix} \quad (4)$$

T_θ is orthogonal, thus the inverse transformation matrix is the transpose of T_θ.

B. DFIG Equations in dq-Form

Applying (4) to (1)-(2) and the other stator and rotor phase equations gives the DFIG dq-model in [pu]:

$$v_{qs} = -\frac{1}{\omega_B}\frac{d}{dt}\psi_{qs} - R_s i_{qs} + \omega\psi_{ds} \qquad (5)$$

$$v_{ds} = -\frac{1}{\omega_B}\frac{d}{dt}\psi_{ds} - R_s i_{ds} - \omega\psi_{qs} \qquad (6)$$

$$v_{qr} = -\frac{1}{\omega_B}\frac{d}{dt}\psi_{qr} - R_r i_{qr} + (\omega-\omega_r)\psi_{dr} \quad (7)$$

$$v_{dr} = -\frac{1}{\omega_B}\frac{d}{dt}\psi_{dr} - R_r i_{dr} - (\omega-\omega_r)\psi_{qr} \quad (8)$$

$$\psi_{qs} = L_{ss}i_{qs} + L_m i_{qr} \qquad (9)$$

$$\psi_{ds} = L_{ss}i_{ds} + L_m i_{dr} \qquad (10)$$

$$\psi_{qr} = L_{rr}i_{qr} + L_m i_{qs} \qquad (11)$$

$$\psi_{dr} = L_{rr}i_{dr} + L_m i_{ds} \qquad (12)$$

In (5)-(8), ω is the rotational speed of the dq-frame, i.e. $\omega = d\theta/dt$ where $\theta = \theta(t)$ is the angle between the d-axis and stator a-axis (Fig. 2); and ω_r is the rotational speed of the rotor, i.e. $\omega_r = d\theta_r/dt$. For the synchronously rotating frame, ω is the synchronous speed, thus in [pu] $\omega = \omega_s = 1$ and $(\omega-\omega_r)$

$= (\omega_s - \omega_r) = s\ \omega_s$ where s is the slip. In (9)-(12), $L_{ss} = L_{self,s} + L_{leak,s} - L_{mut,s}$ and $L_m = L_{sr}$.

IV. DFIG dq-EQUATIONS FOR STABILITY STUDIES

In stability studies, machines are usually represented as a voltage source behind transient impedance. Equations (5)-(12) can be rewritten so that the DFIG is represented as shown in Fig. 3. To this end, stator and rotor fluxes in (5)-(8) are eliminated with (9)-(12), and the following new variables are defined:

$$v_q' = (L_m/L_{rr})\omega_s\psi_{dr} \qquad (13)$$

$$v_d' = -(L_m/L_{rr})\omega_s\psi_{qr} \qquad (14)$$

$$X_s' = \omega_s\left(L_{ss}L_{rr} - L_m^2\right)/L_{rr} \qquad (15)$$
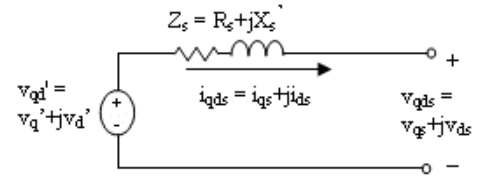
$$T_0' = \omega_s L_{rr}/R_r \qquad (16)$$

Fig. 3. DFIG model for stability studies.

After some substitutions, the DFIG-model in [pu] becomes:

$$\frac{X_s'}{\omega_s\omega_B}\frac{d}{dt}i_{qs} = -\left(R_s + \frac{X_s - X_s'}{T_0'}\right)i_{qs} + X_s'i_{ds}\ \dots$$

$$+ (1-s)v_q' - \frac{1}{T_0'}v_d' - v_{qs} + \frac{L_m}{L_{rr}}v_{qr} \qquad (17)$$

$$\frac{X_s'}{\omega_s\omega_B}\frac{d}{dt}i_{ds} = -X_s'i_{qs} - \left(R_s + \frac{X_s - X_s'}{T_0'}\right)i_{ds}\ \dots$$

$$+ \frac{1}{T_0'}v_q' + (1-s)v_d' - v_{ds} + \frac{L_m}{L_{rr}}v_{dr} \qquad (18)$$

$$\frac{1}{\omega_s\omega_B}\frac{d}{dt}v_q' = \frac{X_s - X_s'}{T_0'}i_{ds} - \frac{1}{T_0'}v_q' + sv_d' - \frac{L_m}{L_{rr}}v_{dr} \quad (19)$$

$$\frac{1}{\omega_s\omega_B}\frac{d}{dt}v_d' = -\frac{X_s - X_s'}{T_0'}i_{qs} - sv_q' - \frac{1}{T_0'}v_d' + \frac{L_m}{L_{rr}}v_{qr} \ (20)$$

$$i_{qr} = -(1/\omega_s L_m)v_d' - (L_m/L_{rr})i_{qs} \qquad (21)$$

$$i_{dr} = (1/\omega_s L_m)v_q' - (L_m/L_{rr})i_{ds} \qquad (22)$$

$$\psi_{qs} = -(1/\omega_s)v_d' + (X_s'/\omega_s)i_{qs} \qquad (23)$$

$$\psi_{ds} = (1/\omega_s)v_q' + (X_s'/\omega_s)i_{ds} \qquad (24)$$

V. Electromagnetic Torque

The instantaneous total active power produced by the DFIG is the sum of stator and rotor active powers:

$$P_{DFIG} = P_s + P_r \qquad (25)$$

where P_s and P_r are the real parts of $v_{qds}.i_{qds}{}^*$ and $v_{qdr}.i_{qdr}{}^*$ respectively. With $v_{qds} = v_{qs}+jv_{ds}$, $i_{qds} = i_{qs}+ji_{ds}$, $v_{qdr} = v_{qr}+jv_{dr}$ and $i_{qdr} = i_{qr}+ji_{dr}$, we have:

$$P_s = v_{qs}i_{qs} + v_{ds}i_{ds} \qquad (26)$$

$$P_r = v_{qr}i_{dr} + v_{dr}i_{dr} \qquad (27)$$

Substituting (5)-(8) in (26)-(27), gives:

$$P_{DFIG} = -R_s\left(i_{qs}{}^2 + i_{ds}{}^2\right) - R_r\left(i_{qr}{}^2 + i_{dr}{}^2\right)\ldots$$
$$-i_{qs}\frac{1}{\omega_B}\frac{d\psi_{qs}}{dt} - i_{ds}\frac{1}{\omega_B}\frac{d\psi_{ds}}{dt}\ldots$$
$$-i_{qr}\frac{1}{\omega_B}\frac{d\psi_{qr}}{dt} - i_{dr}\frac{1}{\omega_B}\frac{d\psi_{dr}}{dt}\ldots$$
$$+\omega_s\psi_{ds}i_{qs} - \omega_s\psi_{qs}i_{ds} + s\omega_s\psi_{dr}i_{qr} - s\omega_s\psi_{qr}i_{dr} \quad (28)$$

The first two terms correspond to the machine losses, the second four terms to the power associated with flux variation, and the last four terms to the airgap power, i.e. the power converted from mechanical to electrical form. The electromagnetic torque T_e is obtained by dividing the airgap power by the mechanical speed of the DFIG rotor. Doing this and using (9)-(12), gives in [pu]:

$$T_e = L_m\left(i_{qs}i_{dr} - i_{ds}i_{qr}\right) \qquad (29)$$

Adding and subtracting the term $(L_mL_{rr}/L_{rr})i_{qs}i_{ds}$ gives the expression of T_e [pu] to be used with the DFIG model (5)-(12):

$$T_e = \left(L_m/L_{rr}\right)\left(i_{qs}\psi_{dr} - i_{ds}\psi_{qr}\right) \qquad (30)$$

Substituting (13)-(14) in (30) gives another equivalent expression of T_e to be used with the DFIG model (17)-(24):

$$T_e = \left(v_d'/\omega_s\right)i_{ds} + \left(v_q'/\omega_s\right)i_{qs} \qquad (31)$$

VI. Drive Train Model

A. Two-Mass Model

If the turbine, gearbox, generator, shafts and other transmission components are modeled as two masses H_t and H_g (with $H_t > H_g$) at the extremities of an equivalent common shaft, it follows from mechanics theory, that:

$$2H_t\frac{d\omega_t}{dt} = T_m - T_{sh} \qquad (32)$$

$$2H_g\frac{d\omega_r}{dt} = T_{sh} - T_e \qquad (33)$$

$$\frac{d\theta_{tw}}{dt} = (\omega_t - \omega_r)\omega_B \qquad (34)$$

where H_t and H_g [s] are the turbine and generator inertia, ω_t and ω_r [pu] are the turbine and DFIG rotor speed, and T_{sh} [pu] is the shaft torque:

$$T_{sh} = K\theta_{tw} + D\frac{d\theta_{tw}}{dt} \qquad (35)$$

In (35), θ_{tw} [rad] is the shaft twist angle, K [pu/rad] the shaft stiffness, and D [pu.s/rad] the damping coefficient.

Substituting (35) in (32)-(33), and recalling $\omega_r = (1–s)\omega_s$, gives the drive train 2-mass model:

$$2H_t\frac{d\omega_t}{dt} = T_m - \left(K\theta_{tw} + D(\omega_t - (1-s)\omega_s)\omega_B\right) \qquad (36)$$

$$-2H_g\omega_s\frac{ds}{dt} = \left(K\theta_{tw} + D(\omega_t - (1-s)\omega_s)\omega_B\right) - T_e \quad (37)$$

$$\frac{d\theta_{tw}}{dt} = (\omega_t - (1-s)\omega_s)\omega_B \qquad (38)$$

where T_e is given in (31).

B. One-Mass Model

If the turbine, gearbox, shafts and generator are lumped together into an equivalent mass H_{tot} [s], the following swing equation in [pu] models the drive train:

$$-2H_{tot}\omega_s\frac{ds}{dt} = T_m - T_e \qquad (39)$$

where T_e is given in (31).

VII. Converter Model

In this paper, the converter connected between the DFIG rotor and the grid consists of two PWM voltage source inverters (VSI) separated by a dc-link as shown on Fig. 4. The grid side converter varies its modulation index m_2 in order to maintain the dc-voltage V_{dc} constant and operates at unity power factor, i.e. only the stator delivers the required reactive power to maintain the terminal voltage (stator voltage); the rotor side converter injects the appropriate rotor voltage so that the DFIG speed is equal to its reference value (determined so that the DFIG extracts the maximum amount of wind power within the limit of the machine). The converters are considered as lossless devices, and the switching dynamics are not modeled since their frequency range is much higher than that of interest in power system stability studies.
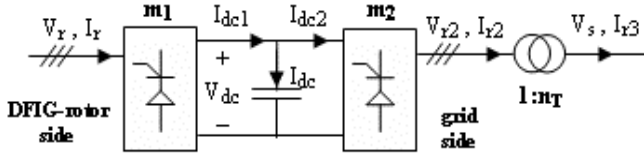
Fig. 4. Back-to-back converter between DFIG rotor and grid.
m_1 and m_2 are modulation index.

In most papers, the dc-link capacitor dynamic is not represented and V_{dc} is assumed as constant. Here, as verification, the differential equation of the dc-capacitor is added to the DFIG model.

To this end, we first establish the relations between ac- and dc-variables of the PWM-VSI shown in Fig. 5. In actual unit, we have [6]:

$$V_{LNrms} = \left(1/2\sqrt{2}\right) m\ V_{DC} \qquad (40)$$

where V_{LNrms} [V] is the ac line-to-neutral rms voltage, m the amplitude modulation ratio, and V_{DC} [V] the dc voltage. The power balance between ac- and dc-sides gives in [VA]:

$$3\ V_{LNrms} I_{rms} = V_{DC} I_{DC} \qquad (41)$$

where I_{rms} [A] is the ac rms current, and I_{DC} [A] the average dc current. Substituting (40) in (41) gives:

$$I_{DC} = \left(3/2\sqrt{2}\right) m\ I_{rms} \qquad (42)$$

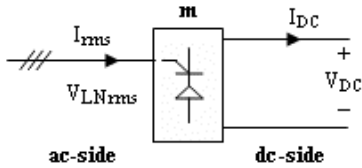

Fig. 5. PWM-VSI with amplitude modulation index m.

In the previous sections the DFIG equations were derived in [pu], thus let us adopt a [pu] notation for the converter equations by defining:

$$V_{dc} = \frac{V_{DC}}{2\sqrt{2}V_{base,1ph}} \qquad (43)$$

$$I_{dc} = \frac{3\ I_{DC}}{2\sqrt{2}\ I_{base}} \qquad (44)$$

where V_{dc} and I_{dc} are in [pu], $V_{base,1ph}$ and I_{base} are the 1-phase base voltage and base current of the DFIG. Thus, for Fig. 4 the following equations in [pu] hold:

$$V_r = m_1 V_{dc} \qquad (45)$$

$$V_{r2} = m_2 V_{dc} \qquad (46)$$

$$I_{dc1} = m_1 I_r \qquad (47)$$

$$I_{dc2} = m_2 I_{r2} \qquad (48)$$

The differential equation of the dc-link capacitor is:

$$I_{dc} = I_{dc1} - I_{dc2} = C\frac{dV_{dc}}{dt} \qquad (49)$$

With (45)-(48), (49) becomes:

$$I_{dc} = \frac{1}{V_{dc}}\left(V_r I_r - V_{r2} I_{r2}\right) = C\frac{dV_C}{dt} \qquad (50)$$

Since $V_s = n_T V_{r2}$ and $I_{r3} = I_{r2}/n_T$, where n_T is the transformer turn ratio (Fig. 4), we have:

$$C\frac{dV_{dc}}{dt} = \frac{1}{V_{dc}}\left(\sqrt{v_{qr}^2 + v_{dr}^2}\sqrt{i_{qr}^2 + i_{dr}^2} - \sqrt{v_{qs}^2 + v_{ds}^2}\,I_{r3}\right) \qquad (51)$$

If the dc-link capacitor dynamics are neglected (V_{dc} constant and $dV_{dc}/dt = 0$), then (51) reduces to the active power balance between rotor and grid side. The current amplitude I_{r3} is derived below.

VIII. INTERFACE WITH THE GRID

To complete the model of the grid connected DFIG, two more algebraic equations have to be added, namely the equations of the active and reactive power exchange between the DFIG and the grid.

A. dq-to-DQ Transformation

The grid voltages and currents are expressed with respect to the reference DQ-frame (slack bus) whereas the DFIG variables are expressed in the machine dq-frame. Thus, when writing the power equations of the grid connected DFIG, transformation from one frame to another should be applied appropriately.

Fig. 7 shows the machine dq-frame with respect to the infinite bus (slack bus) DQ-frame, where δ is the angle between the q- and Q-axis. It is seen that dq- and DQ-variables are related by:

$$v_Q = v_q \cos\delta - v_d \sin\delta \qquad (52)$$
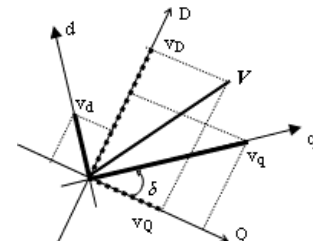
$$v_D = v_q \sin\delta + v_d \cos\delta \qquad (53)$$

Fig. 7. Machine dq-frame with respect to slack bus DQ-frame.

B. Power Flows on the Grid Side

In this paper, the grid is modeled by its Thevenin equivalent, i.e. an infinite bus behind a line reactance X_e, as depicted on Fig. 8. A stronger grid is modeled by a smaller value of X_e (higher short circuit ratio), and vice versa. From Fig. 8, the powers in [pu] drawn by the grid are:

$$P_{tot} = \sqrt{v_{qs}^2 + v_{ds}^2}\, V_b \sin\gamma / X_e \qquad (54)$$

$$Q_{tot} = \left(\left(v_{qs}^2 + v_{ds}^2 \right) - \sqrt{v_{qs}^2 + v_{ds}^2}\, V_b \cos\gamma \right) \Big/ X_e \qquad (55)$$

where γ is the angle between DFIG stator voltage and infinite bus voltage.

In more elaborated power system studies, the power system would be a network of several buses. In that case, the right hand side of (54) and (55) would be given by the power flow equations (PFE) at the DFIG bus.

C. Power Flows on the DFIG Side

Fig. 8 shows the power flows of the grid connected DFIG:

$$0 = -P_{tot} + \left(P_s + P_r - P_{dc} \right) \qquad (56)$$

$$0 = -Q_{tot} + \left(Q_s - Q_T \right) \qquad (57)$$

where Ptot and Qtot are given in (54)-(55); P_s and P_r are given in (26)-(27); P_{dc}, the power flowing through the dc-capacitor during transients, is obtained by multiplying (51) by V_{dc}; Q_s is the imaginary part of $v_{qds}.i_{qds}^*$; and Q_T is the reactive power consumed by the transformer, i.e:

$$Q_s = v_{ds}i_{qs} - v_{qs}i_{ds} \qquad (58)$$

$$Q_T = X_T I_{r3}^2 \qquad (59)$$

$$P_{dc} = \left(\sqrt{v_{qr}^2 + v_{dr}^2}\, \sqrt{i_{qr}^2 + i_{dr}^2} - \sqrt{v_{qs}^2 + v_{ds}^2}\, I_{r3} \right) \qquad (60)$$
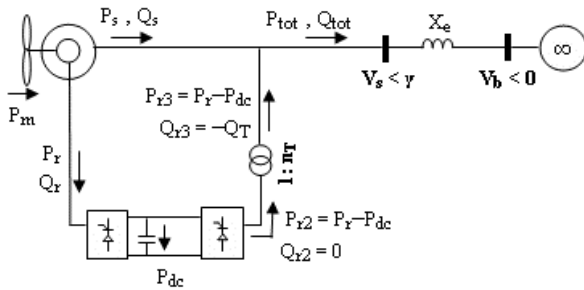
The current amplitude I_{r3} is derived below.

Fig. 8. Power flows of the grid connected DFIG.

D. Current $\bar{I}_{r3}$

The ac-current $I_{r3} \angle \gamma_{Ir3}$ is determined by the Kirchoff current law at the connection point between grid and DFIG. From Fig. 8, this gives:

$$\bar{I}_{r3} = I_{r3} \angle \gamma_{I_{r3}} = \bar{I}_{tot} - \bar{I}_s \qquad (61)$$

where

$$\bar{I}_{tot} = \left(\frac{P_{tot} + jQ_{tot}}{\sqrt{v_{qs}^2 + v_{ds}^2}\, \cos\gamma + \sqrt{v_{qs}^2 + v_{ds}^2}\, \sin\gamma} \right)^* \qquad (62)$$

$$\bar{I}_s = \left(i_{qs}\cos\delta - i_{ds}\sin\delta \right) + j\left(i_{ds}\cos\delta + i_{qs}\sin\delta \right) \qquad (63)$$

with P_{tot} and Q_{tot} given in (54)-(55). In (63) the transformation (52)-(53) was used.

IX. DAE OF THE GRID CONNECTED DFIG

A. Mathematical Background

The mathematical model of a power system can be written as a set of differential algebraic equations (DAE):

$$\frac{dx}{dt} = f(x, z, u) \qquad (64)$$

$$0 = g(x, z, u) \qquad (65)$$

where x, z, and u are the column-vectors of state variables, algebraic variables, and control inputs; f and g are the column-vectors of differential and algebraic equations respectively.

In transient studies, (64)-(65) are solved simultaneously. The solution gives x, z and u in time domain, and allows for the calculation of system outputs:

$$y = h(x, z, u) \qquad (66)$$

where y is the column-vector of outputs and h the column-vector of output algebraic equations.

In small-signal studies, (64)-(65) are linearized around an operation point and the eigenvalue analysis of the A-matrix (defined in the Appendix) allows for the assessment of the system small-signal stability.

In both studies (transient and small-signal), the first step to do is the initialization of the system. This is done in two steps. First, a loadflow is calculated on the grid side by considering the DFIG bus as a PQ or PV bus. Then, with the obtained solution, the DFIG is initialized by solving (64)-(65) with time derivative terms equal to zero and controlled outputs equal to their reference value.

B. Study System DAE

The study system is shown in Fig. 8. The reference Q-axis is aligned with the slack-bus voltage $V_b \angle 0$. Thus, if we align the machine q-axis with the stator voltage $V_s \angle \gamma$, the equations derived in the previous sections can be simplified since:

$$v_{qs} = V_s \qquad (67)$$

$$v_{ds} = 0 \qquad (68)$$
$$\delta = \gamma \qquad (69)$$

where δ is the angle between the q- and Q-axis and γ the angle between DFIG bus and slack bus voltages.

Table I summarizes the DAE of the different grid connected DFIG models for different set of assumptions.

	Model A	Model B	Model C
Assump.	2-mass $(d/dt)_{stator} \neq 0$	1-mass $(d/dt)_{stator} \neq 0$	1-mass $(d/dt)_{stator} = 0$
f(x,z,u)	(17)~(20) (36)~(38) (51)	(17)~(20) (39) (51)	(19)~(20) (39) (51)
g(x,z,u)	(56) (57)	(56) (57)	(56) (57) (17) (18)
h(x,z,u)	(21) (22)	(21) (22)	(21) (22)
x	i_{qs} i_{ds} v_q' v_d' ω_t s θ_t V_{dc}	i_{qs} i_{ds} v_q' v_d' s V_{dc}	v_q' v_d' ω_t s θ_t V_{dc}
z	v_{α} γ	v_{α} γ	v_{α} γ i_{qs} i_{ds}
u	v_{qr} v_{dr}	v_{qr} v_{dr}	v_{qr} v_{dr}
y	i_{qr} i_{dr}	i_{qr} i_{dr}	i_{qr} i_{dr}

For dynamical simulations in the time domain, system and control input models have to be added to the DAE of Table I. Here, the system input is the mechanical torque T_m (which depends on both wind speed and turbine characteristic) and the control inputs are the rotor voltages v_{qr} and v_{dr} (which depend on DFIG control model). Depending on the application (e.g. transient fault analysis), the time-response comparison will indicate which DFIG model to choose (i.e. which assumptions to consider as acceptable).

C. Study System Initialization

If voltage control is provided, the DFIG bus is a PV bus, i.e. P_{tot} and V_s are specified to the grid and the loadflow solution gives Q_{tot} and γ. For the study system of Fig.8, the loadflow equations are simply (54)-(55).

Since the DFIG speed is controlled, the slip s is a controlled output. Thus in steady-state it is equal to its reference value:

$$s_0 = s* \qquad (70)$$

The set point $s*$ depends on the specified power output P_{tot} as follow: if P_{tot} is the nominal DFIG power, the speed is equal to the nominal speed; if P_{tot} is less than the nominal DFIG power, the speed is equal to an optimal value, which depends on the performance characteristic of the turbine C_p, so that the maximum amount of wind power is extracted; i.e.:

$$s* = \begin{cases} s_{nom} & if \quad P_{tot} = P_{nom} \\ s(C_p) & if \quad P_{tot} < P_{nom} \end{cases} \qquad (71)$$

In addition, as the grid-side converter controls the dc-link voltage, V_{dc} is also a controlled output, thus:

$$V_{dc0} = V_{dc}^* \qquad (72)$$

where $V_{dc}*$ is a constant and is given by:

$$V_{dc}^* = \frac{V_{r,ref}}{m_{1,ref}} \qquad (73)$$

In (73), $m_{1,ref}$ is the rotor-side converter modulation index corresponding to the rotor voltage $V_{r,ref}$ [pu] in the reference case (design choice). E.g., to allow enough variation margin, we can choose $m_{1,ref} = 0.75$ for $V_{r,ref} = V_{s,rated}/n$ where $V_{s,rated}$ is the DFIG stator rated voltage and n the DFIG stator-rotor turn ratio.

The remaining 8 variables (i_{qs0}, i_{ds0}, v_{q0}', v_{d0}', ω_{t0}, θ_{tw0}, v_{qr0} and v_{dr0}) are determined by solving f and g simultaneously with zero time derivative terms, controlled outputs as defined above and loadflow solution as obtained above. Since the models of Table I only differ dynamically, their initial operating points (x_0,z_0,u_0) are identical.

For the parameters given in the Appendix, Table II shows some steady-state values corresponding to $P_{tot} = 1$ [pu], $V_s = 1$ [pu], and $s_{nom} = -0.03$ [pu].

	V_{s0}	I_{s0}	V_{r0}	I_{r0}	P_{tot0}	Q_{tot0}	T_{m0}
SG	1	0.9771	0.0255	1.0882	1	0.0113	0.9818
WG	1	0.9843	0.0258	1.1361	1	0.114	0.9776

SG = strong grid (X_e/X_m=0.01), WG = weak grid (X_e/X_m=0.1), $V_{s0} = |v_{sqd0}|$, $I_{s0} = |i_{sqd0}|$, $V_{r0} = |v_{rqd0}|$, $I_{r0} = |i_{rqd0}|$, P_{tot0} and Q_{tot0} = total active and reactive power delivered to the grid, T_{m0} = input mechanical torque.

It is seen that for a weaker grid the reactive power required from the DFIG is substantially larger.

X. SMALL-SIGNAL ANALYSIS

A. Eigenvalues

For the models of Table I, Table III-V show the eigenvalues of their state matrix (see Appendix (A-2)) for the parameters given in the Appendix with $X_e/X_m = 0.01$ (stronger grid). In these tables $\lambda = \sigma \pm j\omega$ are the eigenvalues, $\xi = -\sigma / \sqrt{\sigma^2+\omega^2}$ are the mode damping coefficients, and $f_{osc} = \omega / (2\pi)$ are the mode oscillation frequency.

It is seen that all eigenvalues have real negative parts, thus the system of Fig. 8 is small-signal stable. In Table III, it is seen that the DFIG model with *2-mass* drive train and *with* stator transient, presents three oscillating modes which are high (51.2 Hz), middle (14.9 Hz) and low frequent (2.8 Hz). Comparing Table III and IV shows that in the DFIG model with *one-mass* drive train, the middle frequent oscillating mode (14.9 Hz) disappears. Comparing Table IV and V shows that in the DFIG model *without* stator transients, the high frequent oscillating mode (51.2 Hz) disappears.

Table VI shows the eigenvalues of the DFIG model with *2-mass* drive train and *with* stator transient for $X_e/X_m = 0.1$ (weaker grid). Comparing Table III and VI shows that in a weaker grid the high frequent mode frequency increases (from 51.2 Hz to 57.4 Hz).

TABLE III
EIGENVALUES OF MODEL A WITH Xe/Xm=0.01

A - SG	σ	ω	ξ	f_{osc} [Hz]
λ1	-27.13		1	0
λ2, λ3	-29.53	321.73	0.091	51.2
λ4, λ5	-10.76	93.66	0.114	14.9
λ6, λ7	-6.68	17.37	0.359	2.8
λ8	-27.01		1	0

TABLE IV
EIGENVALUES OF MODEL B WITH Xe/Xm=0.01

B - SG	σ	ω	ξ	f_{osc} [Hz]
λ1	-27.13		1	0
λ2, λ3	-28.86	321.74	0.089	51.2
λ4, λ5	-16.82	24.32	0.569	3.9
λ6	-25.93		1	0

TABLE V
EIGENVALUES OF MODEL C WITH Xe/Xm=0.01

C - SG	σ	ω	ξ	f_{osc} [Hz]
λ1	-27.13		1	0
λ2, λ3	-16.59	23.15	0.582	3.7
λ4	-28.62		1	0

Since the maximum oscillation frequency indicates the minimum simulation time step (STS) to use for the DFIG, it is seen from Table III-V that the STS of the DFIG with 1-mass drive train should be the same as that of the model with 2-mass drive train, whereas the STS of the DFIG model without stator transients can be significantly larger than that with stator transients. From Table VI, it is also seen that when stator transients are represented, the STS should be smaller for a weaker the grid.

TABLE VI
EIGENVALUES OF MODEL A WITH Xe/Xm=0.1

A - WG	σ	ω	ξ	f_{osc} [Hz]
λ1	-39.29		1	0
λ2, λ3	-19.15	360.17	0.053	57.4
λ4, λ5	-11.79	93.72	0.125	14.9
λ6, λ7	-7	17.61	0.369	2.8
λ8	-20.77		1	0

B. Participation factors

Participation factors are calculated with the system matrix and its right and left eigenvectors (see Appendix (A-5)). These factors indicate the normalized contribution of each state variable in the different natural modes of the system.

Table VII shows the result for the DFIG with 2-mass drive train and with stator transient (Model A of Table I). From the columns of Table VII, it is seen that:

- The decaying mode λ_1 is associated with none of the ac state variables, but *only* with the dc state variable V_{dc}.
- The fast oscillating mode (λ_1, λ_2) is *mainly* associated with stator transients (i_{qs}, i_{ds}).
- The middle and low frequent oscillating modes (λ_3, λ_4) and (λ_5, λ_6) are *mainly* associated with drive train transients (ω_t, s, θ_{tw}) and rotor flux q-component transients (v_d' is proportional to ψ_{qr}, see (14)).
- The decaying mode λ_8 is *mainly* associated with rotor flux d-component transients (v_q' is proportional to ψ_{dr}, see (13)).

TABLE VII
PARTICIPATION FACTORS OF MODEL A WITH A STRONG GRID (Xe/Xm=0.01)

0	0.470	0.470	0.030	0.030	0.007	0.007	0.010	x1 = i_{qs}
0	0.442	0.442	0.016	0.016	0.004	0.004	0.006	x2 = i_{ds}
0	0.036	0.036	0.007	0.007	0.018	0.018	0.900	x3 = v_q'
0	0.050	0.050	0.313	0.313	0.204	0.204	0.052	x4 = v_d'
0	0	0	0.010	0.010	0.440	0.440	0.009	x5 = ω_t
0	0.002	0.002	0.446	0.446	0.032	0.032	0.009	x6 = s
0	0	0	0.178	0.178	0.295	0.295	0.014	x7 = θ_{tw}
1	0	0	0	0	0	0	0	x8 = V_{dc}
λ1	λ2	λ3	λ4	λ5	λ6	λ7	λ8	

XI. CONCLUSION

In this paper, different models of the grid connected DFIG were considered (one- or two-mass drive train, with or without stator transients). For each of them, the non-linear differential algebraic equations were established and the initialization of the system was presented. The models were compared with each other with the eigenvalue analysis of their small-signal model.

The main conclusions were that the DFIG model with stator transients and 2-mass drive train presents three oscillating modes (fast, middle and low frequent oscillations of ~50 Hz, ~15Hz and ~3 Hz respectively); dc-link voltage and rotor flux d-component are responsible for decaying modes; stator current, turbine speed, twist angle, generator speed and rotor flux q-component are responsible for oscillating modes; and there is a minimum grid strength under which the DFIG operation is not possible.

XII. APPENDIX

A. System Parameters

DFIG parameters are not readily available, thus in this paper they were defined in terms of ratios.

System Constants		
ωs	1	[pu]
ωB	2π*50	rad/sec
Vb	1	[pu]

System Input		
Tm	1	[pu]

Drive Train		
Ht	3	[sec]
Hg	0.5	[sec]
Htot	3.5	[sec]
K	10	[pu/rad]
D	0.01	[pu*sec/rad]

DFIG		
Rs	0.005	[pu]
Rr	1.1*Rs	[pu]
Xm	450*Rs	[pu]
Lm	Xm/ωs	[pu]
Lss	1.01*Lm	[pu]
Lrr	1.005*Ls	[pu]
n	1.5	[-]

Back-to-back converter		
X_T	0.5	[pu]
C	0.0001	[pu]

Grid		
X_e/X_m	0.01	[pu] for strong grid
	0.1	[pu] for weak grid

B. Linearization and State Matrix

The linearization of (64)-(65) is done by a Taylor series expansion around the operating point (x_0, z_0, u_0) calculated by the system initialization described above. Neglecting terms of order 2 and above, the corresponding linear model is:

$$\frac{d}{dt}\Delta x = A \cdot \Delta x + B \cdot \Delta u \qquad (A\text{-}1)$$

where

$$A = \left[\frac{\partial f}{\partial x} - \frac{\partial f}{\partial z}\left(\frac{\partial g}{\partial z}\right)^{-1}\frac{\partial g}{\partial x}\right]_{x_0, z_0, u_0} \qquad (A\text{-}2)$$

$$B = \left[\frac{\partial f}{\partial u} - \frac{\partial f}{\partial z}\left(\frac{\partial g}{\partial z}\right)^{-1}\frac{\partial g}{\partial u}\right]_{x_0, z_0, u_0} \qquad (A\text{-}3)$$

The matrix A is the system state matrix. Its eigenvalues (real and/or complex) give the natural modes of the system and allow for the assessment of the small-signal stability. If A is real, complex eigenvalues always appear in conjugate pairs.

C. Participation factors

The participation factors of mode i, are given by [8]:

$$p_i = \begin{bmatrix} p_{1i} \\ p_{2i} \\ \dots \\ p_{mi} \end{bmatrix} \qquad (A\text{-}4)$$

where

$$p_{ki} = \frac{|\Phi_{ki}||\Psi_{ik}|}{\sum_{k=1}^{n}|\Phi_{ki}||\Psi_{ik}|} \qquad (A\text{-}5)$$

In (A-4) and (A-5), m is the number of state variables, p_{ki} the participation factor of the kth state variable into mode i, Φ_{ik} the ith element of the kth right-eigenvector of A, Ψ_{im} the mth element of the ith left-eigenvector of A.

XIII. REFERENCES

[1] J.B. Ekanayake, L. Holdsworth, XG. Wu, N. Jenkins, "Dynamic modelling of doubly fed induction generator wind turbines," *IEEE Trans. on Power Sytstems*, vol. 18, pp.803-809, May 2003.

[2] V. Akhmatov, "Modelling of Variable-Speed Wind Turbines with Doubly-Fed Induction Generator in Short-Term Stability Investigations," *3rd Int. Workshop on Transmission Networks for Offshore Wind Farms*, Stockholm Sweden, Apr. 2002.

[3] J.G. Slootweg, H. Polinder, W.L. Kling, "Dynamic modelling of a wind turbine with doubly-fed induction generator," in *Proc. 2001 IEEE Power Eng. Soc. Summer Meeting*, vol. 1, pp 644-649.

[4] S.A. Papathanassiou, M.P. Papadopulos, "State-space modelling and eigenvalue analysis of the slip energy recovery drive," in *IEE Proc. Jan. 1997 - Electr. Power Appl.*, vol. 144, , pp. 27-36.

[5] R. Pena, J.C. Clare, G.M. Asher, "Doubly fed induction generator using back-to-back PWM converters and its application to variable-speed wind-energy generation," in *IEE Proc. May 1996 - Electr. Power Appl.*, vol. 143, No. 3, May 1996.

[6] N. Mohan, *Power Electronics*, 3rd ed., John Wiley & Sons, 2003, p. 228.

[7] D.W. Novotny, T.A. Lipo, *Vector Control and Dynamics of AC Drives*, Oxford Science Publications, 1998.

[8] P. S. Sauer, M. A. Pai, *Power System Dynamics and Stability*, Prentice-Hall 1998.

[9] P. Kundur, *Power System Stability and Control*, Mc Graw Hill 1994.

[10] IEEE committee report, "Recommended phasor diagram for synchronous machines," *IEEE Transactions on Power Apparatus and Systems*, Vol. PAS-88, No. 11, November 1969.

XIV. BIOGRAPHIES

Francoise Mei was born in Ottignies-Louvain-la-Neuve, Belgium, on September 3, 1981. She studied electro-mechanical engineering at the Catholic University of Leuven (K.U.Leuven, Belgium) and graduated in July 2004. She is now working on her Ph.D. at Imperial College London. Her special fields of interest include distributed generation modelling and control.

Bikash C. Pal (M'00–SM' 02) received the B.E.E. (Hons.) degree from Jadavpur University, Calcutta, India, and the M.E. degree from the Indian Institute of Science, Bangalore, India, in 1990 and 1992, respectively. He received the Ph.D. degree from Imperial College London, London, U.K., in 1999. He is presently a Lecturer in the Department of Electrical and Electronic Engineering, Imperial College London. His research interests are in the area of power system dynamics and FACTS controllers.